

Comparison of Mechanical and Tribological Properties of TiN and ZrN Coatings Deposited by Arc-PVD

Michal Kraška (0000-0003-3928-6889)¹, Ladislav Lemberk (0000-0003-4826-3398)², Nikolay Petkov (0000-0002-1971-8341)³, Lucie Svobodová (0000-0001-8661-5150)¹ and Totka Bakalova (0000-0003-2617-0473)¹

¹Faculty of Mechanical Engineering, Department of Material Science, Technical University of Liberec, Studentska 2, 461 17 Liberec, Czech Republic. E-mail: michal.kraska@tul.cz^a, lucie.svobodova@tul.cz^e, totka.bakalova@tul.cz^f

²Institute for Nanomaterials, Advanced Technologies and Innovation, Technical University of Liberec, Studentska 1402/2, 461 17 Liberec, Czech Republic. E-mail: ladislav.lemberk@tul.cz^b

³Central Laboratory of Applied Physics, Bulgarian Academy of Sciences, 61, St. Peterburg Blvd. 4000 Plovdiv, Bulgaria. E-mail: petkovnik@gmail.com^d

The continuous development of thin coatings for different applications and using various coating methods require the characterization of these newly formed surfaces to evaluate their utility properties. Binary thin coatings of titanium (TiN) and zirconium (ZrN) nitrides were prepared using the Arc-PVD (Cathodic Arc Deposition) method. Differences were observed in the structure and morphology of the thin coatings and the change in tribological properties at room and elevated temperatures (150 °C and 300 °C).

The research is focused on evaluating the frictional properties of the coating using the Ball-on-Disc method in the dry friction mode. The emphasis is placed on the resistance of the thin coating to wear. The nanohardness was measured to be 26.2 GPa for TiN and 24.8 GPa for ZrN. Index of resistivity against plastic deformation H^3/E^2 (plastic deformation resistance) for ZrN coating – 0.087 and TiN coating – 0.095, H/E (plasticity index) for ZrN – 0.059 and TiN – 0.060. Better friction properties and wear resistance (at 150 °C) were found for the TiN coating compared to the ZrN coating.

Keywords: Thin coatings (TiN, ZrN); Cathodic arc deposition; Tribological properties; Mechanical properties; Wear resistance

1 Introduction

Nanostructured solids or solid colloids are often prepared in the form of thin coatings. They represent systems formed of nanoparticles with a defined size of 1-100 nm. This range is important because these are substances of a minimal size that can still be considered real surface substances. At the same time, the particle size is not larger than 100 nm, so the development of micro and macrostructures is inhibited. Quantum effects and changes in the behavior of materials are significant within a defined range of size [1, 2]. By developing nanostructured thin films by gradual deposition of atoms/particles, unique physical-mechanical properties of surfaces can be achieved, which are advantageously used in a wide range of industries.

Methods based on the principle of Chemical Vapor Deposition (CVD) and Physical Vapor Deposition (PVD) have been developed for the formation of thin films [3]. One of the most frequently used methods is PVD thermal evaporation and cathodic arc evaporation (Arc-PVD), with almost a century-old history of technical solutions for the production of thin films.

The main advantage of the cathodic arc is the production of highly ionized plasma allowing the formation of a thin coating with high density and very good adhesion to the base material. The main disadvantage of this technology is the creation of so-called droplets. That is, macroparticles adhere to the structure of a thin coating, where residual stresses are likely to arise. Stresses then lead to the chipping of the coating and the formation of craters on the surface [1, 3–5]. Thin films have important applications in mechanical engineering, especially for machining applications [4].

In the tribological process during machining, the material of the friction pairs is degraded by mechanical (abrasion) and chemical-physical (corrosion) influences. In addition to material properties (hardness, microstructure, wettability, etc.), it depends on the environment and machining conditions. Requirements for lower wear rates and lower friction are still pushing the development of coatings with the required properties [6]. In the machining process, for environmental and economic reasons, research has focused on processes without the use of coolants and lubricants [7]. Metal in air, especially in the absence of

lubricants, forms an oxide coating. Its removal by the adhesive-abrasive mechanism and probably by its reformation often play an important role in the process of wear and friction. Ceramic coatings are effective mainly due to low friction and wear, even for operations at elevated temperatures [8]. Oxidation resistance is also a key factor in improving mechanical properties and increasing cutting performance [9]. Due to the high demands on the required properties in the machining process, many types of thin films are constantly being developed.

The first generations of single-coating hard coatings, such as TiN, CrN, ZrN, WC, WC – Co, WC – Ni, ZrCN, and TiCN, have been known since the 1980s. These coatings play an important role due to their high hardness and toughness as well as low coefficients of friction [9, 10]. TiN coatings are commercially used for machine tool surfaces due to their high surface hardness, thermochemical stability, and wear resistance [3–5, 10]. At an elevated temperature of around 250–450 °C, an oxide coating is formed on the TiN surface, and at temperatures higher than ~ 450 °C there is a plastic deformation and coating failure [11] due to oxygen substitution for nitrogen, causing TiO_2 formation leading to phase separation between nitrogen and oxygen [12]. Exposure to higher temperatures can lead to serious damage to machine parts [13].

The research in this work is focused on the evaluation of mechanical and tribological properties of thin films of TiN and ZrN. The methods of nanoindentation, calotest, scratch test, SEM (Scanning Electron Microscopy), confocal microscope, and tribology - Ball-on-Disc (at room and elevated temperatures) were used to evaluate the properties of thin films. The aim is to assess the suitability of the use of newly created coatings for tools for machining purposes. The properties of thin coatings are also assessed on the basis of the relationship between nanohardness (H) and modulus of elasticity (E^*).

The H/E (plasticity index) and H^3/E^2 (plastic deformation resistance) relationships are widely used in the valuable calculation for predicting the development of wear. New coatings with a given hardness H can have significantly different values of elasticity E . Thanks to this, coatings with high elasticity (higher value of H^3/E^2 ratio) resistant to plastic deformation or hard coatings (lower value of H^3/E^2 ratio) with high plastic deformation can be formed. [14]

2 Experimental Procedure

Thin coatings were prepared by Arc-PVD coating on EN ISO HS 6-5-2 tool steel substrate. After cutting, the surface of the substrate samples was ground and polished to ($R_a = 0.01 \mu\text{m}$), and the achieved hardness of the prepared samples was 64–65 HRC [15–

18]. Two variants of thin coatings (binary TiN, ZrN) were prepared for the research.

2.1 Thin coating deposition

Deposition of the nitride coatings was performed at elevated temperatures using cathodes of pure titanium and zirconium (99.99% purity). The samples were mounted in a substrate holder according to the scheme (Fig. 1).

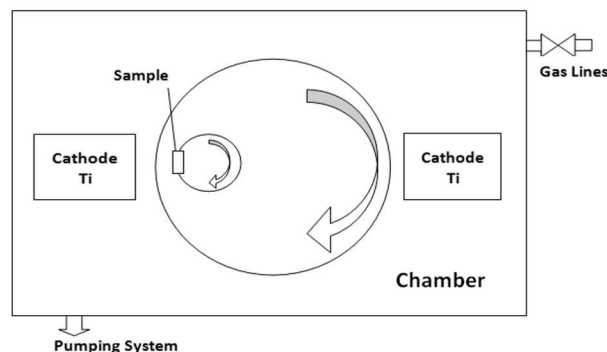


Fig. 1 Scheme of the coating process

Prior to deposition, the following steps were necessary to achieve better adhesion of the coatings to the substrate:

- The substrate was cleaned in an alkaline solution in an ultrasonic bath for 5 minutes, then rinsed with deionized water and dried with boiling ethanol and hot air;
- After the cleaning process, the sample was placed in a vacuum chamber and fixed in a substrate holder;
- The substrate was cleaned in the chamber by bombarding with ions at a voltage of 1000 V and an Ar gas pressure of 0.2 Pa to remove residual contamination traces and oxide coatings;
- In order to increase the adhesion of the coatings to the substrate, an adhesive coating was formed between coating and the substrate (contact interlayer).

For the deposition of TiN coatings, dual cathode of pure Ti was used. The arc current was set to 80 and 70 A, at a voltage (bias) of 80 V. The total deposition time was 100 minutes, N_2 pressure in the vacuum chamber was 0.35 Pa, and the deposition temperature was 300 °C. Ion purification was performed with Ti ions, and the contact interlayer was made of Ti.

For the ZrN coating, only one cathode from pure Zr was used. The arc current was 120 A, negative bias 80 V, deposition time 90 min., N_2 pressure in the vacuum chamber was 0.34 Pa, and deposition temperature 280 °C. Ion purification was performed with Zr

ions, and the contact interlayer was made of Zr.

2.2 Thin coating analysis

A Carl Zeiss Plus Scanning Electron Microscope (SEM) equipped with an EDX (Energy Dispersive Spectroscopy) Oxford instruments energy dispersive spectrometer was used to analyze the chemical composition of the thin coating. To prevent excitation of the signals from the substrate, the low accelerating voltage of the primary electron beam was set to 10 kV. Topographic contrast of secondary electrons (SE) was used to create images of surface morphology; images were taken at an accelerating voltage of 10 kV and a magnification of 5000x. Chemical contrast (backscattered electron, BSE) images were also obtained in cross-sections of the samples to distinguish the distribution of chemical elements.

The height parameters of the surface roughness were obtained using a confocal microscope S Neox 3D according to the ISO 25178 standard. The surface roughness was measured in five different areas on the surface of the studied samples. The size of the scanned area was $850.08 \times 709.32 \mu\text{m}^2$.

Mechanical properties such as nanohardness and modulus of elasticity were determined by a nanoindentation method using CSM Instruments using a Berkovich type diamond tip. During loading and unloading, the device records and analyzes dynamic responses from the penetration of the tip into the material depending on the time and depth of the indentation. The value of the indentation depth for nanoindentation is chosen to be 10% of the thickness of the individual coatings, so that the measured values are not affected by the response from the substrate. The thickness of the coating is measured on the Calotest device equipped with an optical microscope and software; the thickness value needs to be known before the nanoindentation itself.

The adhesion of the coatings to the substrate was evaluated by the scratch method on a Bruker CETR-Universal Materials Tester (CETR-UMT) for Scratch Testing according to EN1071-3: 2005. The device engraved coating with a diamond indenter (Rockwell cone) by constantly increasing the load (2-100 N) while linearly moving the sample perpendicular to the indenter. The scratch test allows you to record changes in normal and tangential forces acting on the

indenter; a graphical record of the acoustic emission (AE), the coefficient of friction (CoF), and the loading force in the Z-axis is also generated during the test. The first and third critical forces (L_{c1} and L_{c3}) were determined according to the record of the scratch path from the optical microscope and the graphical record of the z-axis force, the coefficient of friction, and the acoustic emission. L_{c1} represents the force at which there was an initial indication of coating failure (cohesive failure), and L_{c3} is the force at which complete coating failure occurred (adhesive failure). The equipment used does not allow determining the critical load L_{c2} – spallation (where the coating flakes off, typically at the edges). On each coated sample, four or more measurements were made at different points on the surface with a scratch length of 5 mm.

To test tribological properties, such as wear and friction of contact pairs, the Ball-on-Disc test method, without the use of lubricants, was used on equipment from Anton Paar at room temperature (RT). The principle of the test is to rotate the attached sample (disc), into which the ball is pressed with a specific force for a certain time. Thin-coated samples are used as a "disc," the counterpart is an Al_2O_3 alumina ball with a diameter of 6 mm; the radius of the track during the tribological measurement was set to 8 mm at a constant load of 10 N, 60 RPM over a total distance of 150 m (3000 s). During the tribological test, based on the EN1071-13: 2010 standard, the friction pairs wear out; during the process, the tribometer records dynamic responses, from which CoF and its changes can be evaluated. Samples were also tested at elevated temperatures (ET) using a CETR UMI Multi-Specimen Test System tribometer from Bruker company. The resulting wear of the surface of the friction pairs was evaluated using a confocal microscope.

3 Result

3.1 Chemical composition

The chemical composition of the thin coating elements (TiN, ZrN) was determined by energy dispersion analysis on SEM. The results are shown in Tab. 1. According to the obtained data and within the measurement error, the stoichiometric distribution of the elements of TiN and ZrN is evident.

Tab. 1 SEM/EDX chemical composition analysis of coatings

Coating	Element [at. %]		
	Ti	Zr	N
TiN	49.5	-	50.5
ZrN	-	46.9	53.1

3.2 Surface morphology and coating homogeneity

Images of the surfaces (Fig. 2) show the macroparticles "droplets" and the craters created by their detachment. The adhesion of macroparticles in the

formed coating is typical for Arc-PVD technology. The surface of the coatings, except for craters and droplets, looks homogeneous; there are no other defects. In the section, cracks around the macroparticles and delamination of the coatings were revealed in the coating structure (Fig. 3)

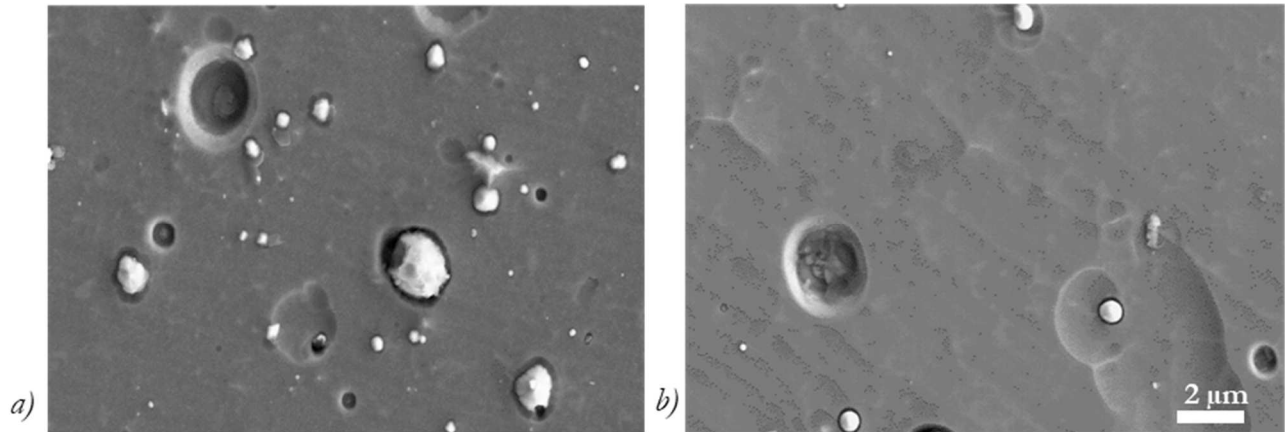


Fig. 2 SEM-SE: Coating surface morphology at 5000 \times magnification a) TiN, b) ZrN (the scale is valid for both images)

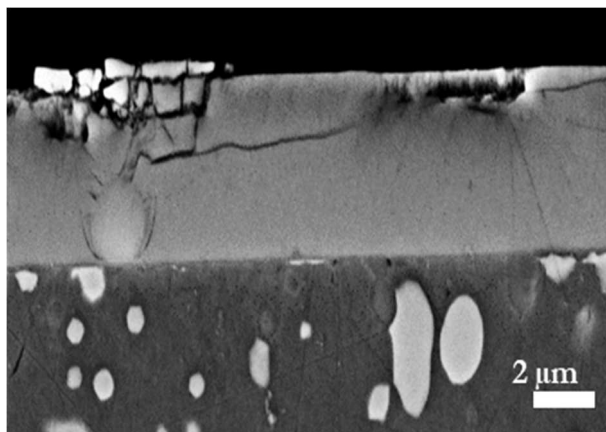


Fig. 3 SEM-SE image, the cross-section of ZrN coating at 5000 \times magnification, 15kV bias

3.3 Surface morphology, parameters, and coating thickness

The average values of height parameters, including the standard deviation, are given in Tab. 2. Sq - average square height of the surface (standard deviation of the height distribution), Sp - largest height of the protrusion (height between the middle plane and the highest protrusion), Sv - largest depth of the depression (height between the lowest depression and the middle plane), Sz - maximum height (height between the lowest depression and the highest protrusion), Sa - average arithmetic height (average surface roughness), Ssk - symmetry of surface heights about mean plane and Sku - measures the sharpness of surface [19].

Tab. 2 Average values and standard deviation of surface parameters

Sample	Surface roughness parameters						
	Sa [nm]	Sz [nm]	Sq [nm]	Sv [nm]	Sp [nm]	Sku [-]	Ssk [-]
Substrate	54.9 \pm 3.3	411.3 \pm 29.2	71.5 \pm 4.0	195.6 \pm 23.4	215.7 \pm 20.6	3.5 \pm 0.3	0.2 \pm 0.2
TiN	66.9 \pm 3.4	761.6 \pm 167.2	90.2 \pm 4.2	228.4 \pm 18.7	533.2 \pm 170.6	7.4 \pm 4.4	1.0 \pm 0.8
ZrN	69.1 \pm 2.9	931.1 \pm 236.0	96.7 \pm 7.2	243.7 \pm 18.0	687.4 \pm 248.4	11.3 \pm 8.2	1.5 \pm 1.1

3.4 Nanohardness and modulus of coating elasticity

The nano hardness (H) and Young's modulus of elasticity (E) were statistically evaluated from the values obtained by nanoindentation (at RT) on a CSM Instruments nanometer hardness tester. Values were obtained as a function of indentation depth ($d = 1/10$

D). Furthermore, the values of the so-called plasticity index (H/E) and the resistance of the material to plastic deformation (H^3/E^2) were calculated from the measured values. The results were statistically processed, and the average values with the standard deviation are given in Table 3.

The thickness of the coatings (D) was evaluated by the calotest method. The average values, including the

standard deviation calculated on the basis of the created intermediate ring (so-called calotte), were recorded in Tab. 3. Coating thickness can affect many

properties of thin coatings. Among other things, its value needs to be known to determine the indentation depth (d).

Tab. 3 Average values and standard deviation of the measured values of nanohardness (H) and modulus of elasticity (E), including calculated values of plasticity index (H/E) and plastic resistivity (H^3/E^2)

Material	D [μm]	d [μm]	H [GPa]	E [GPa]	H^3/E^2	H/E
EN ISO HS 6-5-2	-	0.25	10.3 ± 0.8	274.2 ± 12.3	0.015	0.038
TiN	2.29 ± 0.04	0.23	26.2 ± 1.7	434.7 ± 12.7	0.095	0.060
ZrN	4.54 ± 0.09	0.45	24.8 ± 0.6	417.7 ± 2.5	0.087	0.059

3.5 Evaluation of coating adhesion

The resulting values of the measured critical forces (L_c) determined according to the panoramic and graphical record were statistically processed and recorded in Tab. 4.

Tab. 4 Average values and standard deviation of critical adhesive forces L_{c1} and L_{c3}

Coating	L_{c1} [N]	L_{c3} [N]
TiN	23.3 ± 3.4	74.5 ± 18.5
ZrN	23.6 ± 3.4	70.0 ± 11.0

3.6 Tribological properties and size of friction surface wear

Testing took place in three modes; in an environment at room temperature (RT) and humidity of $24 \pm 2\%$, and at elevated temperatures (ET) of 150°C and 300°C . During the tests, the values of the CoF waveforms were recorded and processed into a graphical form (Fig. 4).

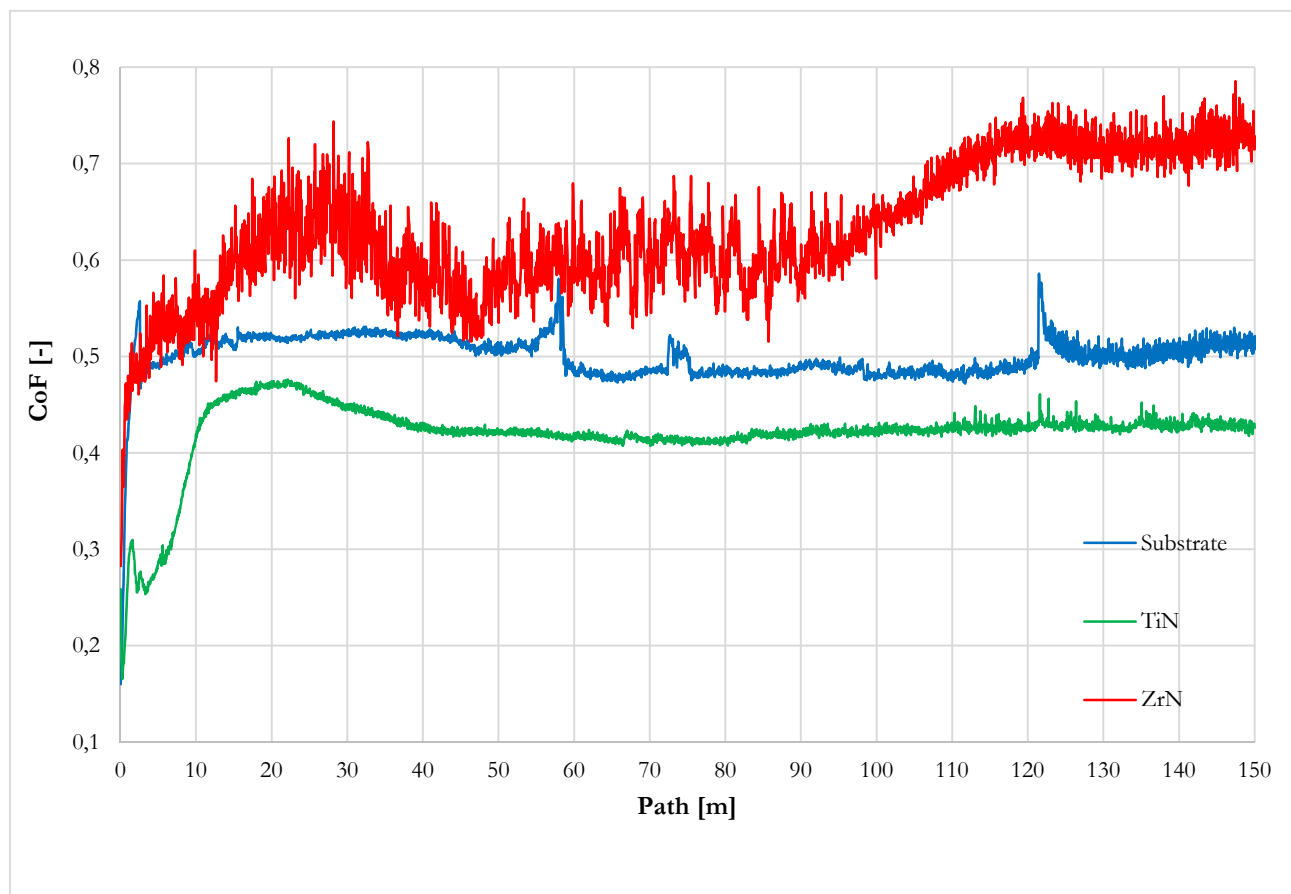


Fig. 4 Recording of CoF dependence on the path at room temperature

The Sensofar metrology S-neox confocal microscope was used to evaluate the amount of wear on the surfaces of the friction pairs. The values of depth and wear width were determined on the scanned surface of the tribological track (disc). The wear of the profile was

assessed in the visually most damaged area (Fig. 5) and subsequently at a distance of 90° axially (4 measurements/sample). The statistically processed data of coating wear (disc) and counterpart of the Al_2O_3 (ball) were recorded in Tab. 5.

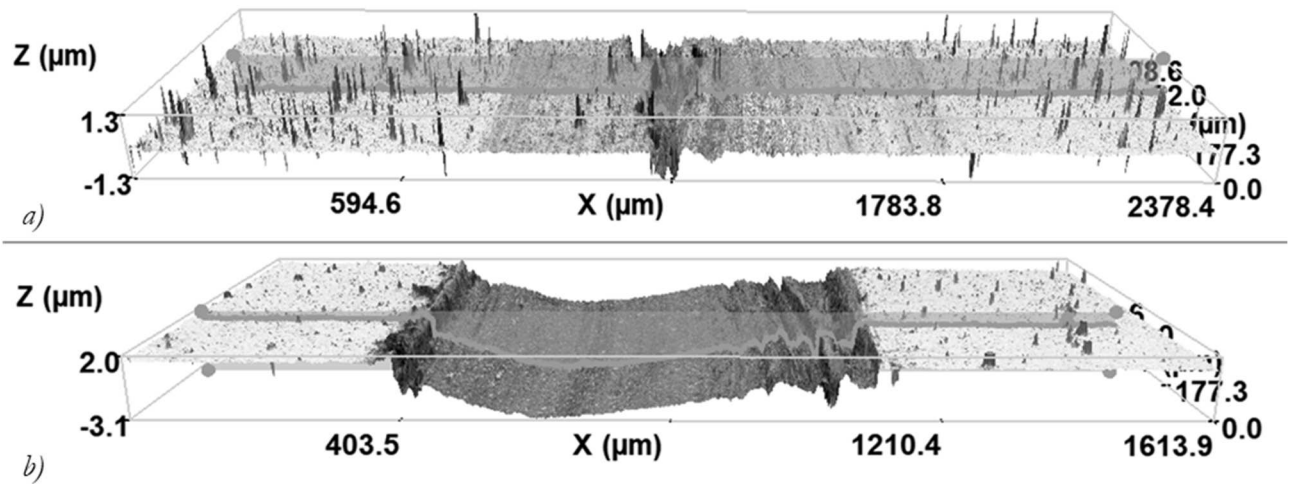


Fig. 5 Wear profile of tribological trace tested at 300 °C: a) local wear zone of TiN thin coating, b) wear of ZrN thin coating

Tab. 5 Average values and standard deviation of friction pair wear

Temperature	Sample	Wear		
		Disk		Counterpart
		Width [μm]	Depth [μm]	[10 ⁻⁴ mm ³]
RT	Substrate	292.1 ± 8.3	0.3 ± 0.0	2.4
	TiN	287.0 ± 19.6	0.3 ± 0.0	2.5
	ZrN	1057.4 ± 7.5	5.9 ± 0.4	232.0
150 °C	Substrate	420.3 ± 4.5	2.6 ± 0.2	3.9
	TiN	309.6 ± 18.9	0.2 ± 0.0	2.3
	ZrN	757.7 ± 4.9	3.6 ± 0.4	59.6
300 °C	Substrate	753.9 ± 4.7	3.7 ± 0.6	5.2
	TiN	1105.2 ± 4.3	1.8 ± 0.6	4.7
	ZrN	888.8 ± 10.4	4.3 ± 0.3	29.5

4 Discussion of results

Thin coating samples were prepared by cathodic arc deposition (Arc-PVD). The method used is characterized by the formation of macroparticles (so-called droplets). Probably the concentration of residual stresses in places of occurrence of droplets leads to a violation of the cohesion between the droplet and base coating, which leads to the release of droplets and the formation of so-called "craters". Apart from the mentioned defects (Fig. 2), no other defects were visible on the surface of monitored coatings. Defects in the form of delamination's in about 1/2 to 2/3 of the coating thickness from surface and around droplets were visible in the section. However, this could be caused by cutting the sample by releasing the internal stress and mechanically damaging the thin coating. Macroparticles are observable on the surface of both coatings (Fig. 2); macroparticles in the structure were observed mainly in the ZrN coating (Fig. 3). It is clear how the macroparticle has grown since the beginning

of the deposition and the gradual development of macroparticles during the entire coating deposition is also observable in the image [20-25]. Macroparticles formed during the deposition in the coating structure can adversely affect the overall properties of the substrate-coating system. However, there are deposition methods to reduce them [26-29].

Mechanical properties such as nanohardness and modulus of elasticity were evaluated by nanoindentation. High nanohardness values of 25 GPa for ZrN and 26 GPa for TiN were measured. It is important that the tool steel EN ISO HS 6-5-2 is supplied as standard in the annealed state; after the heat treatment by hardening, the surface hardness is increased to 65 HRC. The subsequent coating increases the hardness against the hardened surface to 241% ZrN and 254% TiN, which ensures significantly greater surface wear resistance. The reduced modulus of elasticity of 274 GPa was measured for the steel substrate. For the coatings, values are 418 GPa for ZrN and 435 GPa for TiN, which is an increase in the modulus of elasticity

by 53-58 % over the substrate surface. From the measured values of nanohardness and modulus of elasticity of the coatings, important indicators were calculated, the so-called plasticity index H/E and the index expressing the resistance to plastic deformation H^3/E^2 (Tab. 4). H/E (0.015) and H^3/E^2 (0.038) values were calculated for the steel substrate. For the thin coatings, H/E values of 0.059 (ZrN) and 0.060 (TiN) and H^3/E^2 values of 0.087 (ZrN) and 0.095 (TiN) were calculated [30-34]. Adhesion of thin coatings to the substrate is almost identical (Tab. 5). Critical forces L_{c1} and L_{c3} are high enough for machining purposes.

Tribological properties such as wear and friction were investigated at room (RT) and elevated temperatures ($E_T = 150\text{ }^\circ\text{C}$ and $300\text{ }^\circ\text{C}$). Due to the nature of the thin coating as a protection of the substrate (against wear, corrosion, etc.), the depth of wear can be considered more significant. After the substrate is exposed, the thin coating may lose its significance of the monitored parameters. For this reason, wear results are evaluated based on the depth of damage of the coatings. For comparison, the depth of wear was related to the coating thickness, and it was found that the RT wear was up to 13 % TiN. This wear can be considered to be of little severity (in relation to the depth of wear). Considering the above height parameters (Tab. 3), the height irregularities of the surface

were basically "smoothed out" and slightly deepened (TiN). The depth of wear is similar to the Sv parameter (Tab. 3). The ZrN coating was completely damaged (131 %). Numerous macroparticles in the surface could have caused a greater degree of wear and also had an effect on increasing the surface roughness. The wear of the Al_2O_3 counterpart against TiN was similar to that against the substrate. Against ZrN, the wear was much higher (Tab. 6). The effects of other counterpart materials on CoF have been studied in [35].

Exposure to elevated temperatures has led to a significant difference in wear. At $150\text{ }^\circ\text{C}$, there was slight damage to TiN thin coating up to 8 % of the thickness, and ZrN thin coating was up to 80 %. As can be seen, the increased temperature of $150\text{ }^\circ\text{C}$ has the effect of mitigating the damage against RT, especially in the TiN coating, but also for Al_2O_3 counterparts (Tab. 6). At $300\text{ }^\circ\text{C}$ significant damage occurred. TiN thin coating damage increased to 79 %, and ZrN thin coating to 94 %. Especially for TiN thin coating, the damage was not uniform along the tribological path. Damages were concentrated in the local zones (Fig. 5a), and a powerful abrasive damage mechanism is observable. Therefore, high values of the standard deviation of the damage must be considered. For the uncoated substrate, the damage after exposure to $300\text{ }^\circ\text{C}$ was 12× greater than RT.

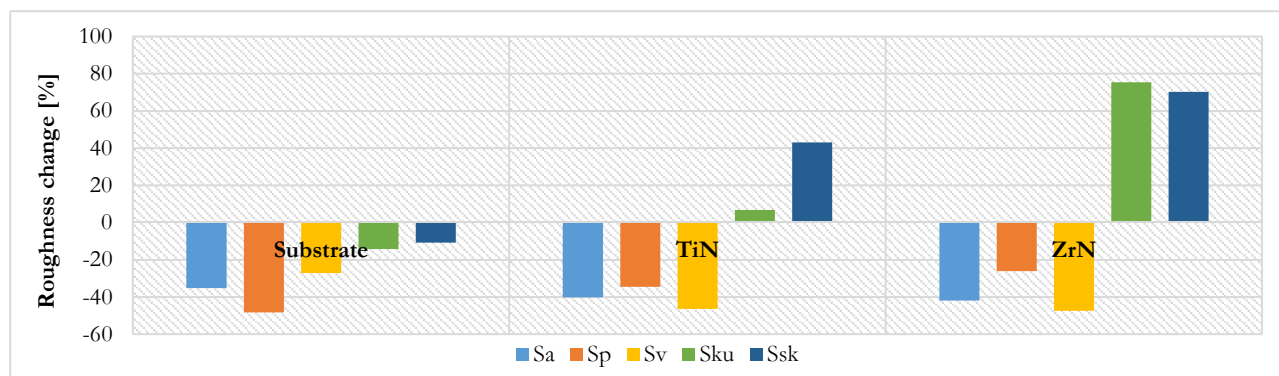


Fig. 6 Change in surface roughness parameters after exposure to $150\text{ }^\circ\text{C}$

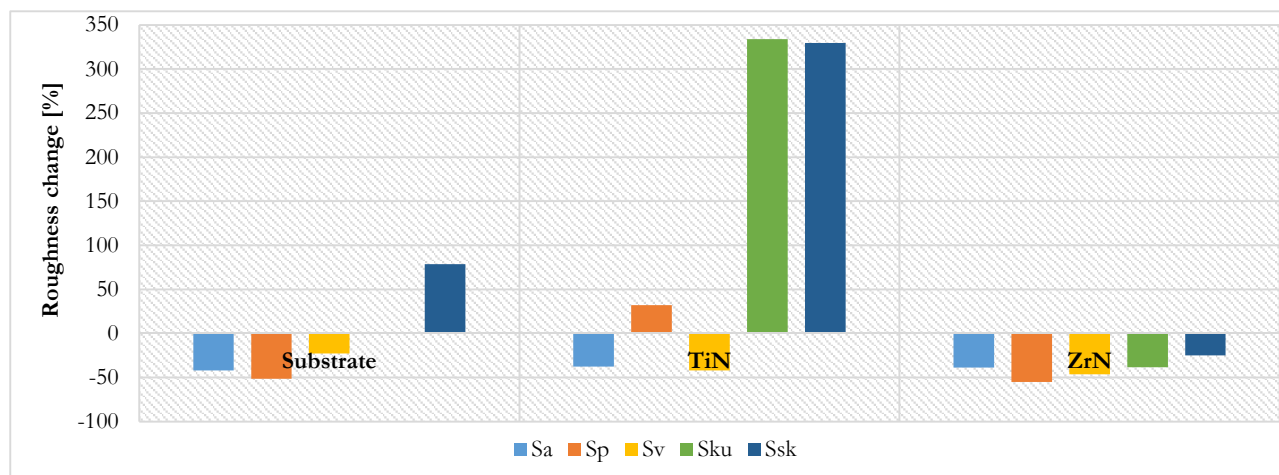


Fig. 7 Change in surface roughness parameters after exposure to $300\text{ }^\circ\text{C}$

Surface roughness is a key property in relation to friction and wear processes. Both coatings (TiN and ZrN) have high values of protrusions (Sp) and surface kurtosis (Sku) at RT. Higher surface roughness, especially the size of the protrusions (Sp), can affect the CoF values (by reducing the contact area) and also affect the abrasive effect during the friction process. Breaking off a hard protrusion from the surface can damage the coating and cause a significant increase in CoF. After exposing the samples to elevated temperature during the tribological experiment and subsequent cooling, the height parameters of the surface roughness were analyzed (Tab. 3). The increased temperature (150 and 300 °C) caused changes in the morphology of the coating surfaces. The plots in Fig. 6 and Fig. 7 express the percentage change in surface roughness parameters measured at RT relative to those after exposure to higher temperatures. From the plots, it can be seen how after exposure of the coatings to elevated temperatures, there was essentially a "smoothing" of the surface (Sa, Sp, Sv) for both thin coatings, including the substrate. However, for the TiN coating, there was an increase in protrusions (Sp) at 300 °C. A significant increase in the skewness (Ssk) and kurtosis (Sku) parameters is also probably related to this. The high density of surface spiking is clearly visible in Fig. 5a on the surface next to the tribological trace, where many pointed peaks are visible. A strange phenomenon is a change in the height parameters of the ZrN coating. At 150 °C, a more pronounced change in surface roughness was observed compared to surfaces at 300

°C. Changes in surface morphology (a dramatic increase in Sku and Ssk parameters) can affect the friction and wear processes of thin coatings. Coatings that do not undergo significant changes in surface morphology when the temperature increases could indicate their thermal stability.

Mean CoF values at RT ranged from 0.45 (TiN) to 0.65 (ZrN). At 150 °C, it ranged from 0.2 (TiN) to 0.45 (ZrN), and at 300 °C from 0.94 (ZrN) to 1.15 (TiN). For the TiN coating at RT, the stable CoF versus substrate behavior is clearly visible from the plot (Fig. 4). In contrast, a strong instability can be seen for ZrN. In the significant increases in CoF, the distance at which this coating was destroyed can be estimated. For the substrate, a so-called stick slip effect occurred. The high CoF value of TiN at 300 °C could be due to the high content of decomposed hard coating products in the tribological trace (by compaction). High wear and CoF can also be affected by oxidation, as described in the introduction [11]. More generally, high CoF values, especially above 1.0 (Fig. 8), can be caused by various principles (quantum effects, physico-chemical bonds, mechanical locks, etc.) [35]. It is obvious that an elevated temperature of around 300 °C is disadvantageous, especially for TiN thin coating. Elevated temperatures are more favourable for ZrN thin coating than room temperatures, yet coating damage is still high (Fig. 8). By properly setting the coating process and predeposition preparation, thin coatings can be obtained to improve the utility of base material properties.

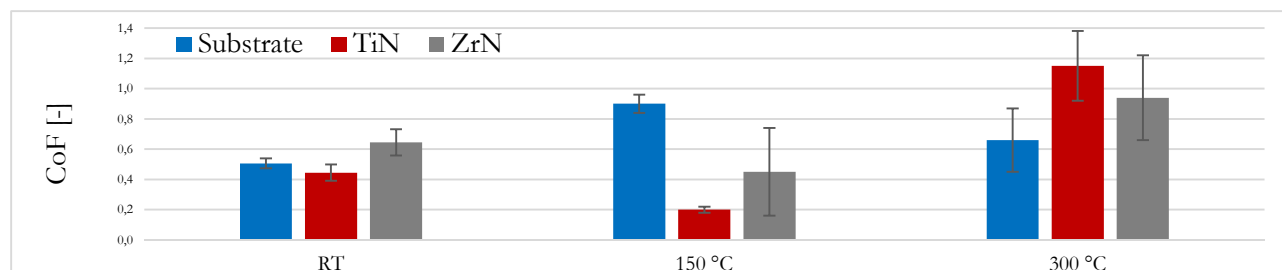


Fig. 8 Average values and standard deviations of CoF measured during a 150 m path with a corundum counterpart at different temperatures in dry friction mode

Defects in the coatings can have an adverse effect on frictional processes when thin coatings are used on the surfaces of contact parts. The hard particles of the coating between the friction pair in the tribological process act as an abrasive; the resulting damage may be more pronounced than with the uncoated substrate. An exemplary example of an unsuitable coating under given conditions is the ZrN coating, which was completely damaged by a tribological test at room temperature. The depth of damage to the coating and the counterpart was more than 20 times and 95 times, respectively, greater than that of uncoated steel. It should be noted that the thickness of this coating was

~ 2 times greater than TiN because different deposition parameters were used [36]. The large difference in the thickness of the coatings could strongly influence the measurement of adhesion values. An adequate procedure would be to optimize the deposition parameters to achieve a similar thickness of coatings.

5 Conclusion

The coatings are coated with good homogeneity in a stoichiometric ratio. They show good adhesion values and high values of nanohardness and modulus of elasticity. In the tribological test, the substrate was detected only in the ZrN at room temperature (the

integrity of the thin coating was broken). Also, the most resistant coatings suitable for applications in adhesive-abrasive environments (such as machining) can be recognized with coatings with the highest values, especially resistance to plastic deformation (H^3/E^2), plasticity index (H/E), adhesive forces; also coatings with smaller thicknesses show higher durability. However, it depends on the conditions of the use of thin coatings. It is especially evident in the TiN at 300 °C. The ZrN coating with extensive surface damage also showed extensive wear of the counterpart. It is obvious how necessary is to respect the conditions of use of coatings. The best results for dry friction conditions were achieved at 150 °C for the TiN coating, which showed very low values of friction coefficient and surface wear.

Acknowledgments

This work was supported by the Student Grant Competition of the Technical University of Liberec under project No. SGS-2022-5060 and by the project "Pretreatment, coating and protection of the substrate", registration number CZ.01.1.02/0.0/0.0/20_321/0025264 were obtained through the financial support of the Ministry of Industry and Trade in the framework of the targeted support of the "Application VIII", the Operational Programme Enterprise and Innovations for Competitiveness.

References

- [1] J. FIALA A I. KRAUS, *Povrchy a rozhraní*. 2016
- [2] L. BARTOVSKÁ A M. ŠIŠKOVÁ, *Fyzikální chemie povrchu a koloidních soustav*. Praha: Vysoká škola chemicko-technologická, 2005
- [3] V. SEDLÁČEK, *Povrchy a povlaky kovů*. Praha: CVUT, 1992
- [4] K. DADOUREK, *Vybrané technologie povrchových úprav*. Liberec: Technická univerzita v Liberci, 2007
- [5] J. KOSKINEN, „Cathodic-Arc and Thermal-Evaporation Deposition”, in *Comprehensive Materials Processing*, Elsevier, 2014, s. 3–55. doi: 10.1016/B978-0-08-096532-1.00409-X
- [6] HASEGAWA, T. (2008). Tribology research trends. Nova Science Publ.
- [7] E. LUGSCHEIDER, O. KNOTEK, C. BARIMANI, A H. ZIMMERMANN, „Arc PVD-coated cutting tools for modern machining applications”, *Surf. Coat. Technol.*, roč. 94, s. 641–646, 1997
- [8] T. BAKALOVA, P. LOUDA, L. VOLESKÝ, K. BORŮVKOVÁ, A L. SVOBODOVÁ, „Nanoadditives SiO₂ and TiO₂ in Process Fluids”, *Manuf. Technol.*, roč. 15, č. 4, s. 502–508, 2015
- [9] A. HÖRLING, L. HULTMAN, M. ODÉN, J. SJÖLÉN, A L. KARLSSON, „Mechanical properties and machining performance of Ti1-xAlxN-coated cutting tools”, *Surf. Coat. Technol.*, roč. 191, č. 2–3, s. 384–392, 2005
- [10] A. RAZMI A R. YEŞILDAL, „Microstructure and Mechanical Properties of TiN/TiCN/TiC Multilayer Thin Films Deposited by Magnetron Sputtering”, 2018
- [11] S. WILSON A A. T. ALPAS, „Effect of temperature and sliding velocity on TiN coating wear”, *Surf. Coat. Technol.*, roč. 94–95, s. 53–59, říj. 1997, doi: 10.1016/S0257-8972(97)00475-1
- [12] N. MADAOU, N. SAOULA, B. ZAID, D. SAIDI, A A. S. AHMED, „Structural, mechanical and electrochemical comparison of TiN and TiCN coatings on XC48 steel substrates in NaCl 3.5% water solution”, *Appl. Surf. Sci.*, roč. 312, s. 134–138, 2014
- [13] M. ALI, E. HAMZAH, A M. R. TOFF, „Friction coefficient and surface roughness of TiN-coated HSS deposited using cathodic arc evaporation PVD technique”, *Ind. Lubr. Tribol.*, 2008
- [14] A. LEYLAND A A. MATTHEWS, „On the significance of the H/E ratio in wear control: a nanocomposite coating approach to optimised tribological behaviour”, *Wear*, roč. 246, č. 1–2, s. 1–11, 2000
- [15] T. BAKALOVA, N. PETKOV, H. BAHCHEDZHIEV, P. KEJZLAR, A L. VOLESKÝ, „Monitoring Changes in the Tribological Behaviour of CrCN Thin Layers with Different CH₄/N₂ Gas Ratios at Room and Elevated Temperatures”, *Manuf. Technol.*, roč. 18, č. 4, s. 533–537, 2018
- [16] T. BAKALOVA, N. PETKOV, T. BLÁŽEK, P. KEJZLAR, P. LOUDA, A L. VOLESKÝ, „Influence of Coating Process Parameters on the Mechanical and Tribological Properties of Thin Films”, in *Defect and Diffusion Forum*, 2016, roč. 368, s. 59–63
- [17] T. BAKALOVA, N. PETKOV, H. BAHCHEDZHIEV, P. KEJZLAR, A P. LOUDA, „Comparison of mechanical and tribological properties of TiCN and CrCN coatings deposited by CAD”, *Manuf. Technol.*, roč. 16, č. 5, s. 859–864, 2016
- [18] T. BAKALOVA, N. PETKOV, H. BAHCHEDZHIEV, P. KEJZLAR, P. LOUDA, A M. ĐURÁK, „Improving the tribological and mechanical properties of an

- aluminium alloy by deposition of AlSiN and AlCrSiN coatings", *Manuf Technol*, roč. 17, s. 824–830, 2017
- [19] T. BAKALOVA, P. LOUDA, L. VOLESKY, A. Z. ANDRŠOVÁ, „The use of optical microscopy to evaluate the tribological properties", *Manuf. Technol.*, roč. 14, č. 3, s. 256–261, 2014
- [20] M. POHLER, R. FRANZ, J. RAMM, P. POLCIK, A. C. MITTERER, „Cathodic arc deposition of (Al,Cr)2O3: Macroparticles and cathode surface modifications", *Surf. Coat. Technol.*, roč. 206, č. 6, s. 1454–1460, pro. 2011, doi: 10.1016/j.surfcoat.2011.09.028
- [21] A. S. KUPRIN *et al.*, „Structural, mechanical and tribological properties of Cr-V-N coatings deposited by cathodic arc evaporation", *Tribol. Int.*, roč. 165, s. 107246, led. 2022, doi: 10.1016/j.triboint.2021.107246
- [22] D. M. HOLZAPFEL, Z. CZIGÁNY, A. O. ERIKSSON, M. ARNDT, A. J. M. SCHNEIDER, „Thermal stability of macroparticles in Ti0.27Al0.21N0.52 coatings", *Appl. Surf. Sci.*, roč. 553, s. 149527, ervenec 2021, doi: 10.1016/j.apsusc.2021.149527
- [23] Y. VENGESA, A. FATTAH-ALHOSSEINI, H. ELMKHAH, A. O. IMANTALAB, „Influence of post-deposition annealing temperature on morphological, mechanical and electrochemical properties of CrN/CrAlN multilayer coating deposited by cathodic arc evaporation- physical vapor deposition process", *Surf. Coat. Technol.*, roč. 432, s. 128090, nor 2022, doi: 10.1016/j.surfcoat.2022.128090
- [24] A. DELGADO, O. GARCIA-ZARCO, J. RESTREPO, A. S. E. RODIL, „AlCrVN coatings deposited by cathodic arc: friction and wear properties evaluated using reciprocating sliding test", *Surf. Coat. Technol.*, s. 128140, led. 2022, doi: 10.1016/j.surfcoat.2022.128140
- [25] A. W. BAOUCHI A. A. J. PERRY, „A study of the macroparticle distribution in cathodic-arc-evaporated TiN films", *Surf. Coat. Technol.*, roč. 49, č. 1, s. 253–257, pro. 1991, doi: 10.1016/0257-8972(91)90064-4
- [26] A. I. RYABCHIKOV, P. S. ANANIN, A. E. SHEVELEV, S. V. DEKTYAREV, D. O. SIVIN, A. A. I. IVANOVA, „Joint influence of steered vacuum arc and negative repetitively pulsed bias on titanium macroparticles suppression", *Surf. Coat. Technol.*, roč. 355, s. 240–246, pro. 2018, doi: 10.1016/j.surfcoat.2018.02.047
- [27] J. KOURTEV, R. PASCOVA, A. E. WEIBMANTEL, „Arc evaporated TiN films with reduced macroparticle contamination", *Thin Solid Films*, roč. 287, č. 1, s. 202–207, jen 1996, doi: 10.1016/S0040-6090(96)08751-2
- [28] D. A. KARPOV, „Cathodic arc sources and macroparticle filtering", *Surf. Coat. Technol.*, roč. 96, č. 1, s. 22–33, lis. 1997, doi: 10.1016/S0257-8972(98)80008-X
- [29] J. SALAMANIA *et al.*, „Influence of pulsed-substrate bias duty cycle on the microstructure and defects of cathodic arc-deposited Ti1-xAlxN coatings", *Surf. Coat. Technol.*, roč. 419, s. 127295, srp. 2021, doi: 10.1016/j.surfcoat.2021.127295
- [30] Y. KONG, X. TIAN, C. GONG, A. P. K. CHU, „Reprint of “Enhancement of toughness and wear resistance by CrN/CrCN multilayered coatings for wood processing”", *Surf. Coat. Technol.*, roč. 355, s. 318–327, pro. 2018, doi: 10.1016/j.surfcoat.2019.06.042
- [31] X. FU, L. CAO, C. QI, Y. WAN, A. C. XU, „Ultralow friction of PVD TiN coating in the presence of glycerol as a green lubricant", *Ceram. Int.*, roč. 46, č. 15, s. 24302–24311, jen 2020, doi: 10.1016/j.ceramint.2020.06.211
- [32] B. WARCHOLINSKI, A. GILEWICZ, A. S. KUPRIN, A. I. V. KOLODIY, „Structure and properties of CrN coatings formed using cathodic arc evaporation in stationary system", *Trans. Nonferrous Met. Soc. China*, roč. 29, č. 4, s. 799–810, dub. 2019, doi: 10.1016/S1003-6326(19)64990-3
- [33] W. CUI, F. NIU, Y. TAN, A. G. QIN, „Microstructure and tribocorrosion performance of nanocrystalline TiN graded coating on biomedical titanium alloy", *Trans. Nonferrous Met. Soc. China*, roč. 29, č. 5, s. 1026–1035, kvě. 2019, doi: 10.1016/S1003-6326(19)65011-9
- [34] T. PLICHTA, R. ZAHRADNICEK, A. V. CECH, „Surface topography affects the nanoindentation data", *Thin Solid Films*, roč. 745, s. 139105, bř. 2022, doi: 10.1016/j.tsf.2022.139105
- [35] Y. TANNO A. A. AZUSHIMA, „Effect of counter materials on coefficients of friction of TiN coatings with preferred grain orientations", *Wear*, roč. 266, č. 11–12, s. 1178–1184, 2009
- [36] A. VERESCHAKA *et al.*, „Investigation of the influence of the thickness of nanolayers in wear-resistant layers of Ti-TiN-(Ti,Cr,Al)N coating on destruction in the cutting and wear of carbide cutting tools", *Surf. Coat. Technol.*, roč. 385, s. 125402, bř. 2020, doi: 10.1016/j.surfcoat.2020.125402